

# 3D Printed Flexible Capacitive Force Sensor with a Simple Micro-Controller Based Readout

Martijn Schouten, Remco Sanders and Gijs Krijnen  
 Robotics And Mechatronics group  
 University of Twente  
 Enschede, The Netherlands  
 m.schouten-1@alumnus.utwente.nl

**Abstract** - This paper describes the development of a proof of principle of a flexible force sensor and the corresponding readout circuit. The flexible force sensor consists of a parallel plate capacitor that is 3D printed using regular and conductive thermoplastic poly-urethane (TPU). The capacitance change due to an applied sinusoidal force is measured using an LCR meter. A proof of principle, using an oscillatory readout circuit consisting of only an operational amplifier and a frequency-counter based on an Arduino Nano, is provided. This indicates the possibility to implement low-cost capacitive sensors into 3D printed objects, which is especially interesting for customised robotic and prosthetic applications.

*Keywords* - Capacitive Sensors; Elastomer; TPU, 3D printing; Force sensor; Fused Deposition Modeling

## I. INTRODUCTION

3D printed sensors can easily be customised and therefore might find use in custom products in for example medical or sports applications. Also since complexity is cheap in additive manufacturing, it may become economically interesting to use the technique to fabricate complex robotic systems. Due to today's availability of flexible filaments, dielectric as well as electrically conductive, it now becomes possible to 3D print flexible sensors of all kinds, e.g. for soft robotic applications.

In relation to this work Saari et al. earlier described a 3D printed force sensor that used an elastomer as dielectric and stiff electrodes fabricated from copper wires embedded during printing [1]. Another 3D printed capacitive sensor that used wires as electrodes has been fabricated by Shemelya et al. [2]. However, 3D printed flexible capacitive sensors have not been presented in literature yet.

### A. Sensing principle

The force sensors described in this work are based on the measurement of the change in capacitance in between two flexible conductors, see Fig. 1. The change in capacitance arises due to the fact that the material is flexible and therefore will be easily deformed when a force is applied.

The capacitance of the sensor can be approximated by two parallel plates with a flexible dielectric in between. Since the

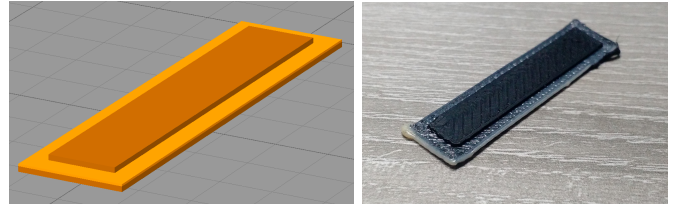


Fig. 1. Left: a CAD drawing of the proposed sensor used to print the sensor. Right: a picture of the actual sensor

distance between the plates is much smaller than the dimensions of the electrodes (6.4 mm x 36 mm versus 0.2 mm), the capacitance can be calculated using the parallel plate approximation. Data of generic thermoplastic polyurethanes suggest that the Poisson's ratio of polyurethane is close to 0.5 [3]. Therefore when the dielectric is compressed the area of the electrodes increases, such that the total volume ( $V$ ) of polyurethane will roughly stay the same, leading to:

$$C = \frac{\epsilon_r \epsilon_0 A}{d} = \frac{\epsilon_r \epsilon_0 V}{d^2} \quad (1)$$

where  $A$  is the area of the plates,  $d$  is the distance in between the plates,  $\epsilon_r$  is the relative dielectric constant of the dielectric,  $\epsilon_0$  is vacuum permittivity and  $C$  is the capacitance of the sensor. For small changes around an initial area  $A_0$  and an initial thickness  $d_0$  the change in capacitance is found from the partial derivative of  $C$  with respect to  $d$ :

$$\Delta C = \left. \frac{\partial C}{\partial d} \right|_{d \rightarrow d_0} \Delta d = -2 \frac{\epsilon_r \epsilon_0 A_0}{d_0^2} \Delta d \quad (2)$$

Note that the change in capacitance for this in-compressible dielectric is twice as large as for a compressible dielectric, since the area of the capacitor plates also changes. In the situation where the material is used in its linear range, the following equation can be used

$$\Delta d = -\frac{F d_0}{A_0 E'} \quad (3)$$

Where  $E'$  is the effective Young's modulus of the material in this situation where it is placed in between two stiffer electrodes and  $F$  is the compressive force that is applied. When (3) is combined with (2), a relation for the expected

This work was developed within the SoftPro project, funded by the European Union's Horizon 2020 Research and Innovation Programme under Grant Agreement No. 688857

capacitance change is obtained.

$$\Delta C = \frac{2\epsilon_r\epsilon_0}{d_0E'}F \quad (4)$$

Therefore in the linear regime there is no dependence of the capacitance change on the capacitor area. At last, since both the dielectric constant and thickness of the material are not known accurately, using (1) a convenient expression is obtained:

$$\frac{\Delta C}{C} = \frac{2}{AE'}F \quad (5)$$

## II. METHODOLOGY

### A. Sensor fabrication

The sensors are printed using a Flashforge Creator Pro printer that is equipped with a Flexion extruder from Diabase Engineering, in order to be able to print flexible filaments. The dielectric consists of Flexion X60 Ultra-Flexible Filament by MakeShaper. The electrodes are made from 85-700+ PI-ETPU filament kindly supplied by Palmiga Innovations.

Both materials are printed with a 100% infill at a layer height of 100  $\mu\text{m}$ . An image of the CAD model used to print the sensors can be found in Fig. 1. In this image light orange indicates X60 and dark orange PI-ETPU.

The thickness of respectively the bottom electrode, the dielectric and the top electrode are 500  $\mu\text{m}$ , 200  $\mu\text{m}$  and 500  $\mu\text{m}$ . The size of the top electrode in the CAD file is 36 x 6.4 mm and the size of the bottom electrode is 40 x 10 mm

### B. Measurement setup

The sensor is mounted in a sample holder which is laser cut out of Delrin, see Fig. 2 for a drawing and Fig. 3 for a picture of the measurement setup. The sensor is tested by applying a well defined force using a linear actuator (SMAC LCA25-050-15F) and monitoring the capacitance. The actuator is configured to load the sensor with a combination of a constant plus a sinusoidal force since no negative forces can be applied with this setup and it has to be kept in place.

### C. Sensor read-out

The fabricated sensors have been interrogated in two ways: by an LCR meter for accurate characterisation and by an Arduino based read-out to demonstrate the possibility for a low-cost sensor-interface.

1) *Read-out by LCR meter:* The sensor was characterised using an HP4842a LCR meter operating at a frequency of 25 kHz and a voltage of 1 V. It was configured for a 4 wire

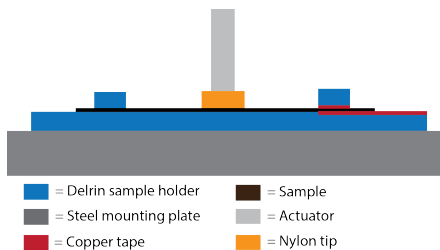


Fig. 2. A schematic representation of the measurement setup



Fig. 3. The measurement setup

measurement and therefore is connected to the sample using 4 shielded cables. The cores of the two cables of the high and the two cables of the low side are connected near the measurement setup. The grounds of all four cables are also connected near the measurement setup. The capacitance measured by the LCR meter when only the cables are connected is less than 1 pF.

2) *Oscillator and frequency counter:* As a proof of principle a readout circuit has been built using an Astable Op-amp multi vibrator circuit (Fig. 4). The oscillation frequency of this oscillator can be calculated using the following equation [4]:

$$f_0 = \frac{1}{2R_1C \ln\left(\frac{1+\beta}{1-\beta}\right)} \quad \text{with } \beta = \frac{R_3}{R_2 + R_3} \quad (6)$$

Combining (5) and (6) it can be shown that in the ideal case of no parasitic capacitances the fractional resonance frequency change is given by:

$$\frac{\Delta f_0}{f_0} = -\frac{2}{AE'}F \quad (7)$$

hence giving a linear relation between relative oscillation frequency and force.

The oscillation frequency of the multivibrator is determined by using an Arduino Nano, which contains an Atmega328 from Atmel. One of the Atmega328's 8-bit counter's is programmed such that it uses the multivibrator's output signal as a clock. Every 400  $\mu\text{s}$  the oscillation frequency is calculated based on the number of periods that were observed by the 8-bit counter. The capacitance of 50 calculations (20 ms) is averaged in order to filter out as much 50 Hz noise as possible.

## III. RESULTS

### A. Basic sensor characteristics

The resistance between the bottom and the top electrode was measured to be 80 M $\Omega$ . The resistance from one side of the

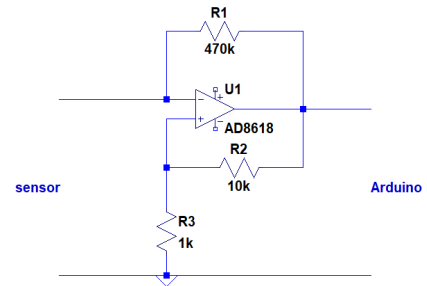


Fig. 4. The Astable Op-amp multivibrator

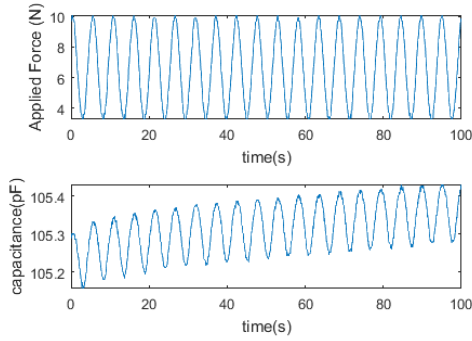


Fig. 5. Sinusoidal force excitation (top) and sensor response (bottom) as measured by an LCR meter

bottom electrode to the other end showed  $10\text{ k}\Omega$ . The resistance of the top electrode was  $20\text{ k}\Omega$ .

### B. Capacitive measurements

1) *LCR meter*: Fig. 5 shows the response of the LCR meter at a sinusoidal excitation of  $0.2\text{ Hz}$ . In Fig. 6 the capacitance of the sensor is plotted against the force applied to the sensor. The colour in this plot corresponds to the time axis in figure 5. The Signal-to-noise and distortion ratio (SINAD) of the measured capacitance is  $19.7\text{ dB}$ . The Signal-to-Noise Ratio (SNR), when excluding the drift by not taking into account signals below  $0.05\text{ Hz}$ , is  $38\text{ dB}$ .

2) *Arduino based readout circuit*: Fig. 7 shows the capacitance of the sensor as measured by the read-out circuit build with an Arduino and an op-amp when the sensor is excited with a sinusoidal force. An estimate of the parasitic capacitance of the readout circuit can be obtained by comparing the data in Fig. 7 and Fig. 5, since the parasitic capacitance of the LCR meter is negligible. This indicates a parasitic capacitance of  $38\text{ pF}$ . The SINAD of the measured capacitance is  $12.8\text{ dB}$ . The SNR, when excluding the drift by not taking into account signals below  $0.05\text{ Hz}$ , is  $28\text{ dB}$ .

## IV. DISCUSSION AND CONCLUSION

The measured capacitance change is  $160\text{ fF}$  at a change in force of  $6.6\text{ N}$ . When no pressure is applied the sensor has a capacitance of  $105.22\text{ pF}$  for a top electrode area of  $2.3\text{ cm}^2$ . According to (5) these values correspond to an effective

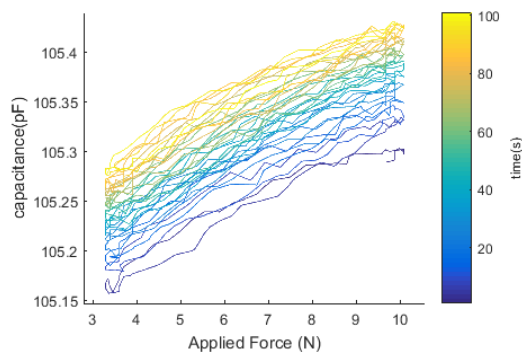


Fig. 6. The capacitance plotted against the applied force

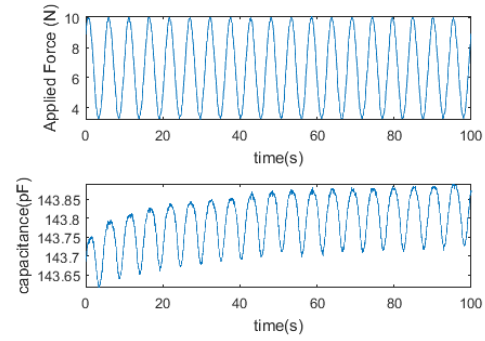


Fig. 7. Response of the sensor at a sinusoidal excitation, measured using the Arduino based readout circuit

Young's modulus of  $38\text{ MPa}$ , which is high compared to an estimate of the Young's modulus of X60 based on its shore hardness of  $60\text{ A}$  [6], which is  $3\text{ MPa}$  [5]. This high value could be caused by the restricted lateral expansion of the X60 due to the relative stiffness of the electrodes or by the anisotropy of the 3D printed material. If this is the case the sensitivity of the sensor might be increased by printing the dielectric using a lower infill percentage, in order to reduce the Poisson ratio of the dielectric and benefit from density modulation.

The results obtained using the LCR meter also show that the sensors drift. This drift might at least partially be explained by the creep of the material as a result of the DC-offset in the force.

The micro-controller based readout circuit has a smaller SINAD and SNR than the LCR meter. However the observed noise suggests that sub Newton forces may be measured. To improve the read-out signal the parasitic capacitance may be reduced and a commercial capacitance to digital converter chip might be used. Finally it should be noted that a possible effect of the resistance of the electrodes on the measured capacitance can not yet be ruled out.

In conclusion we have shown a 3D printed flexible capacitive force sensor with cost-effective read-out sensor that may have a high potential for use in soft robotic and prosthetic devices. Due to its flexibility and the ease by which it can be made in large surfaces it may possibly be applied as artificial tactile skin in soft robotics.

## REFERENCES

- [1] M. Saari, B. Xia, B. Cox, P. S. Krueger, A. L. Cohen, and E. Richer, "Fabrication and Analysis of a Composite 3D Printed Capacitive Force Sensor," *3D Printing and Additive Manufacturing*, vol. 3, no. 3, pp. 136–141, September 2016.
- [2] C. Shemelya, F. Cedillos, E. Aguilera, D. Espalin, D. Muse, R. Wicker, and E. MacDonald, "Encapsulated copper wire and copper mesh capacitive sensing for 3-d printing applications," *IEEE Sensors Journal*, vol. 15, no. 2, pp. 1280–1286, Feb 2015.
- [3] H. Qi and M. Boyce, "Stress-strain behavior of thermoplastic polyurethanes," *Mechanics of Materials*, vol. 37, no. 8, pp. 817 – 839, 2005.
- [4] (2017). [Online]. Available: <http://www.electronics-tutorials.ws/opamp/op-amp-multivibrator.html>
- [5] (2017). [Online]. Available: [http://www.dowcorning.com/content/publishedlit/11-3716-01\\_durometer-hardness-for-silicones.pdf](http://www.dowcorning.com/content/publishedlit/11-3716-01_durometer-hardness-for-silicones.pdf)
- [6] (2017). [Online]. Available: <https://flexionextruder.com/shop/x60-ultra-flexible-filament-black/>